An EM Transistor Based Brain-Processor Interface

R. Sklyar

Verchratskogo st. 15-1, Lviv 79010 Ukraine, sklyar@tsp.lviv.ua

ABSTRACT

The design and mathematical description of an biomagnetic array of electromagnetic transistors (EMTs) which are ordered in the memristor architecture is advanced. EMT circuit is analysed taking into account the nonlinear inductance of its core. It was shown that the noise can be effectively cancelled by synthetic higher-order gradiometers and such noise cancellation is independent of the noise character or sensor orientation. Considering, EMT as some kind of a memristor gives us the possibility to compose the matrix by nanowires for the biomagnetic programming.

Keywords: biomagnetic field, electromagnetic transistor, array, matrix, gradiometer, memristor, field-programming

1 INTRODUCTION. THE IMPLANTABLE AND EXTERNAL NEUROINTERFACES

Implantable neural probes are generally preferred to have a minimum footprint as possible to minimize neural damage and to facilitate easy entry and movement through the brain tissue. The above requirement combined with the growing interest to undertake neuroscience studies from deeper regions of the brain has necessitated the need to develop ultra-long probes (lengths longer than 5mm) with thicknesses less than 50µm. Such high aspect ratio structures pose a great design challenge as the probes have to be able to withstand the insertion axial forces, retraction forces, and tension forces of the brain tissue.

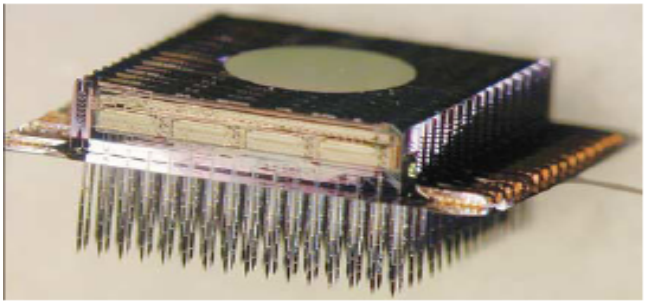

Figure 1: Photo of a 3-D 1024-site 128-channel neuroelectronic interface.

To date, a wide range of neural electrodes have been used in basic neuroscience and neural prosthetic research (brain machine interfaces) starting with the early electrolyte-filled micropipettes [1]. More recently, polymeric microprobes have received a great deal of attention owing to their simple fabrication process, flexibility and biocompatibility to develop hybrid neural probes which have the combined capability to record electrical activity as well as specific neural biochemical markers.

Implantable neural probes for neuroscience and brain machine interfaces are generally preferred to have a minimum footprint as possible to minimize neural damage (Fig.1). Different biocompatible polymers are used to cover the metal and silicon region of the probes to form a biocompatible interface between the probe and the brain tissue.

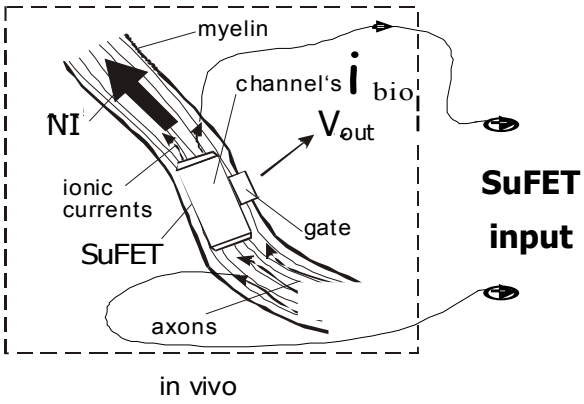

Figure 2: The inclusion of a SuFET device into the nerve fibre or neuronal tissue.

Alternatively, a SuFET based neurotransducer with carbon nanotubes (CNT) or pickup coil (PC) kind of input circuit for the nerve and neuron impulse (NI) has been designed [2]. A nanoSuFET with a high-temperature superconducting channel is introduced into the nerve fibre or brain tissue for transducing their signals in both directions (Fig. 2).

On the other hand, the development of multiple or superconducting quantum interference device (SQUID) has led to an acceleration of research on MEGs an external system for the brain, which arranged around the head. The MEG is produced from the whole volume of the neural stimulus throughout the brain and is configured for a 3-D measurement [3]. The mechanical stimulation to the

right index finger produces signals which, by Faraday's Law should be related by a time derivative and and orthogonal relationship in space (Fig. 3).

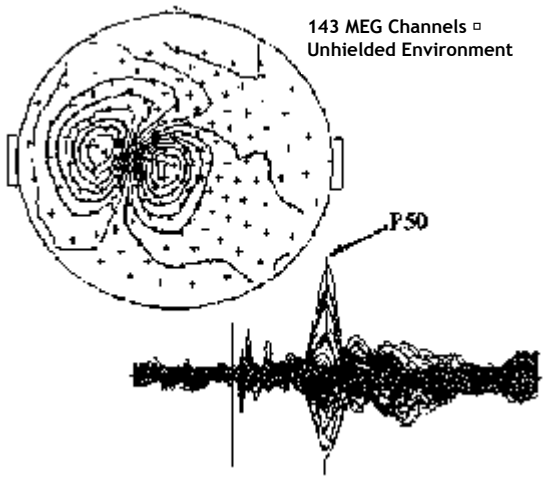

Figure 3: Plan view of a human head with the MF distribution.

Most SQUIDs are incorporated into whole-head systems for magnetoencephalography (MEG)- the detection of MFs produced by brain. A typical helmet contains about 300 sensors, including a number of reference sensors for noise cancellation, cooled to 4.2 K. The sensors are generally configured as first order gradiometers, measuring either an axial or off-diagonal gradients [4].

2 CIRCUIT PARAMETERS OF EMT

A further step should be synthesis of the said two methods in order to develop the external (non-implantable) brain machine interface. Human being from whom EM signals are to be extracted is the subject, which is attached with EM sensor and the raw EM signal is acquired. The EM sensors are surface PCs, which are used in regular configuration where PCs with a small distance between each other are positioned within the helmet type surface to pick up the local signals within the place of interest. The problem of sensing the EM signal for amplification/switching it with a speed of light in a single solid-state device (EMT) has been advanced [2]. The said problem in the advanced method is solving by application of ferroelectric or ferroelectromagnetic (FE or FEM) crystals which are controlled by an electric or magnetic fields (EF or MF) respectively [5]. The device for controlling (amplifying, switching, logical comparison) of a magnetic flux in the processing crystal is designed with an application of ferromagnetic material with an unique fashion dependence between its magnetic permeability B and the strength of MF H. Also controlling the device by both EF and MF allows matching it with the previous stages.

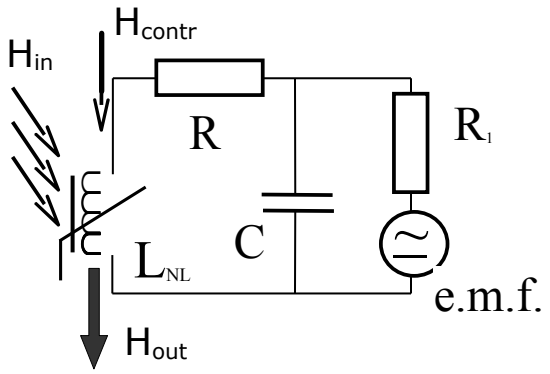

Figure 4: An equivalent circuit of EMT with the nonlinear inductance and control e. m. f.

The nonlinear element in the EMT circuit is an inductance L_{NL} which is formed by the control coil and FE/ FEM processing body (Fig. 4). The FM materials are characterised by the dependence of magnetic inductance B from a MF strength H, which named as magnetized curve. The L_{NL} is defined by the dependence of magnetic flow engagement $\psi=\omega\Phi$ from the current in a winding of driving coil I_m. This dependence is displayed along a sloping main magnetized curve of a wide hysteresis loop which can be approximated by a non-linear function with reference to the running point b [6]:

$$B= b_1H + b_2H^3 + b_3H^5 \quad (1)$$

The equivalent complex resistance of L_{NL} is:

$$\underline{Z_L}=\frac{\dot{U}_m}{\dot{I}_m}=j\omega L(1-\frac{3}{4}kI_m^2) \quad (2)$$

For the EMT's device shown as a complex replacing circuit (Fig. 4) we can written down the complex resistance:

$$\underline{Z}(j\omega, I)=R+j[\omega L(1-kI^2)-\frac{1}{\omega C}] \quad (3)$$

The dependence of a module of the first harmonic from frequency is following:

$$I=\frac{U}{Z}=\frac{U}{R\sqrt{1+Q^2[\omega(1-kI^2)-\frac{1}{\omega_0}]}} \quad (4)$$

According to the method of phase plain is possible to investigate the transfer function B=f(H) in view on transfer processes, possibilities of appearance the resonances and

NSTI-Nanotech 2009, www.nsti.org, ISBN 978-1-4398-1783-4 Vol. 2, 2009

unstable states. One phase trajectory can be constructed by a delta-method.

3 THE SPACE PLACEMENT AND ARRAY DISTRIBUTION

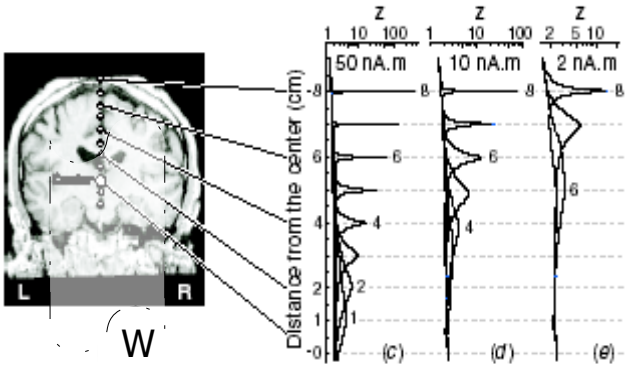

Figure 5: The peak width of a three dimensional source under the MEG sensor array W.

The term 'magnetoencephalography (MEG) sensor array' will mean the collection of EMTs (Fig. 5). Rejection of environmental noise can be improved by measuring a magnetic field difference, rather than the field itself. Such flux transformers are referred to as gradiometers (i.e. the field difference approximates a component of the field gradient tensor) [7]. The radial gradiometer detects the radial gradient of a radial magnetic field (radial with respect to the surface of the head) (Fig 6).

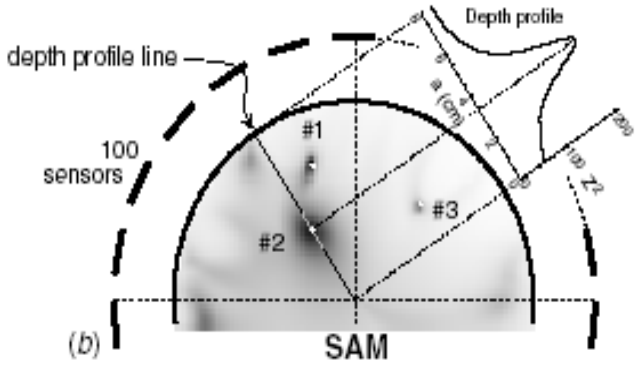

Figure 6: Synthetic aperture magnetometry(SAM) is a class of beamformer where the scan is performed in 4D space.

The 20 cm^2 array for sheathing of the brain consists of 40 thous. EMTs which could be produced by printed electronics processes. These elements are set out into the square or rectangular matrice A_{ij} and take part in further mathematical operations (Fig. 7). Control (and interaction) signals can be both in the current and voltage form to create MF or EF respectively. Signal contribution corresponding to a dipole of a specified rms amplitude and at a specified position within the model sphere, figure 5, was added to the noise covariance matrix and the resulting covariance matrix was used to compute SAM depth profiles.

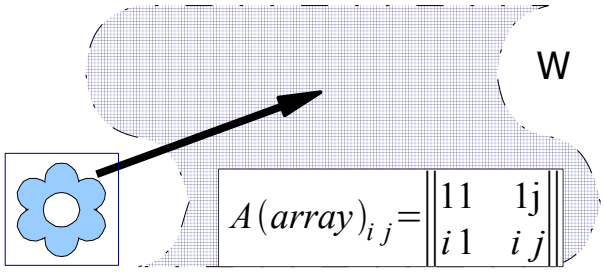

Figure 7: Location of each EMT on flex former W and relevant matrix for its further processing.

4 THE INTERFACE MATRIX AND ARRANGEMENT OF NANOELEMENTS

On a basis of the acquired Eqs. (2-4), which are the defined the characteristics of the elements in a circuit (Fig. 4), it is possible to define the input-output dependence for a nonlinear control coil. A matrix equation for the output value of H_{out} takes the form:

$$\dot{B} = A_2 H_{out} + B_2 V \quad \text{or} \quad \begin{bmatrix} u_m \\ i_m \end{bmatrix} = \begin{bmatrix} \frac{1}{R} & 0 \\ 0 & R_1 \end{bmatrix} \begin{bmatrix} u_c \\ i_L \end{bmatrix} \quad (5)$$

After substitution of Eqs. (2-4) the final signal processing matrix (Eq. 5) for a control e. m. f. element with the internal resistance R_1 is completed. This equation of state matrix can normally be resolved by analytical or digital methods. The most widespread and simple method is Euler's digital integration for a step-by-step computation.

4.1 The Memristor Interconnections Nanowires

A memristor is a 2-terminal thin-film electrical circuit element that changes its resistance depending on the total amount of charge that flows through the device. This property arises naturally in systems for which the electronic and dopant equations of motion in a semiconductor are coupled in the presence of an applied electric field. Our EMT device can expand this ability by an applied MF.

The first feasibility demonstration for the integration and operation of nanoscale memristor crossbars with monolithic on-chip FETs has been presented [8]. In this case, the memristors were simply used as 2-state switches (ON and OFF, or switch closed and opened, respectively) rather than dynamic nonlinear analog device to perform

wired-logic functions and signal routing for the FETs; logical AND is represented by multiplication and OR by addition. A proof-of-principles are provide validation that the same devices as EMTs in a nanoscale circuit can be configured to act as logic, signal routing and memory, and the circuit can even reconfigure itself.

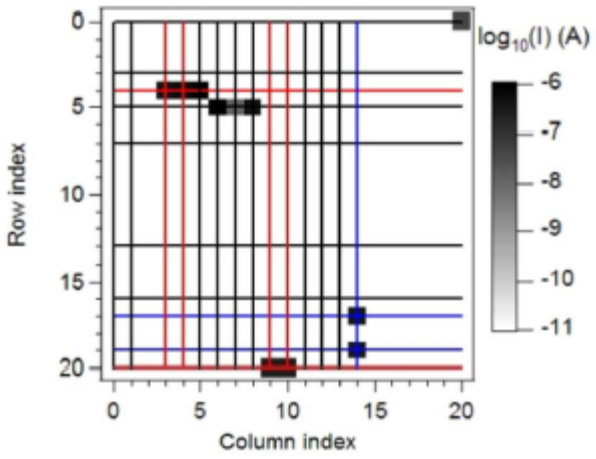

Figure 8: Map of the conductance of the memristors in the crossbar. The squares display the logarithm of the current through memristor at a 0.5-V bias.

Fig. 8 displays in various colors the nanowires in the crossbar selected from those that were determined to be good and the conductance map for the programmed-ON memristors. The gray-scale squares display the current through the individual memristors upon the application of a test voltage of 500-mV bias.

4.2 MF-Programmable Architecture

The processing matrix is a subject for control by MF according to the advanced method. A general hybrid architectural approach named FPNI (field-programmable nanowire interconnect) that trades off some of the speed, density and defect-tolerance of CMOL in exchange for easier fabrication, lower power dissipation, and greater freedom in the selection of nanodevices in the crossbar junctions has been presented [9]. The key difference in FPNI architectures that logic is done only in CMOS, routing only in the nanowires. This significantly reduces static power dissipation, and allows us to use linear (or approximately linear) antifuses for the nanowire junctions. In addition, the FPNI routing network is buffer-based, not inverter-based, which simplifies the routing.

The CMOL (Fig. 9, left column) places a nanowire crossbar on top of a sea of CMOS inverters. The crossbar is slightly rotated so that each nanowire is electrically connected to one pin extending up from the CMOS layer. Selected junctions (shown in green in the bottom panel) are configured as nonlinear resistors or EMTs to implement wired-OR logic (in conjunction with a pull-down transistor in the CMOS), with the CMOS inverters providing gain and inversion.

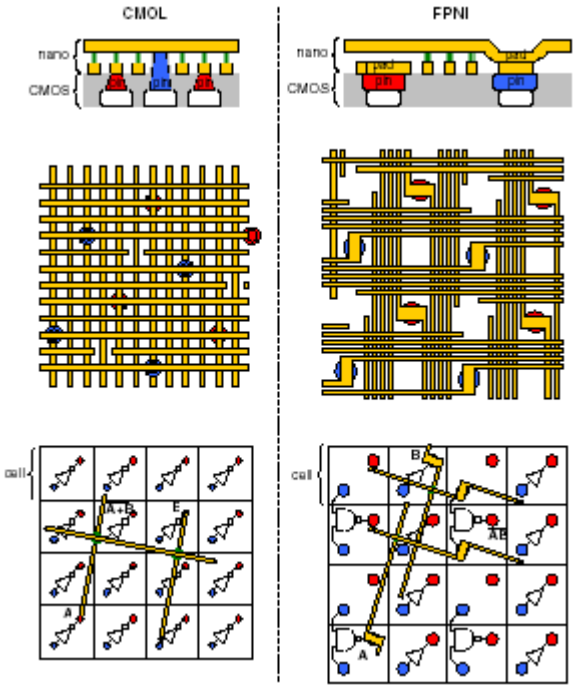

Figure 9: Schematic diagrams of hybrid circuits.

Electrically configured, nonlinear antifuses (green, bottom panel) allow wired-OR logic to be implemented, with CMOS supplying gain and inversion. The FPNI (right column) places a sparser crossbar on top of CMOS gates and buffers.

REFERENCES

[1] M. HajjHassan, V. Chodavarapu, and S. Musallam, Sensors, vol. 8, pp. 6704-6726, 2008.

[2] R. Sklyar, in: Nanotechnology 2008: Life Sciences, Medicine, and Bio Materials, Nano Science & Technology Institute, Cambridge, MA, USA, CRC Press, vol. II, Nano Medicine & Neurology, 810 pages.

[3] G. J. Mapps, Sens. and Actuat. A, vol. 106, pp. 321-325, 2003.

[4] R. Klainer, D. Koelle, F. Ludwig et al., Proc. of the IEEE, vol. 92, pp. 1534-1548, 2004.

[5] R. Sklyar, Patent UA 76691, Bull. 9, 2006.

[6] T. A. Tatur, "The Fundumentals of the Theory of Electrical Circuits", Moscow: Vysshaya shkola, 149-155, 1980.

[7] J. Vrba and S. E. Robinson, Supercond. Sci. Technol., vol. 15, pp. R51–R89, 2002.

[8] J. Borghetti, Zh. Li, J. Straznicky, et al., PNAS,vol. 106, no. 6, pp. 1699–1703, 2009.

[9] G. S. Snider and R. S. Williams, Nanotechnology vol. 18, 035204 (11pp.), 2007.